ICES Journal of Marine Science

ICES Journal of Marine Science (2019), 76(6), 1882–1892. doi:10.1093/icesjms/fsz040

Original Article

Amplifier linearity accounts for discrepancies in echo-integration measurements from two widely used echosounders

Alex De Robertis [1†], Christopher Bassett [1†], Lars Nonboe Andersen[2], Ivar Wangen[2], Scott Furnish[1], and Michael Levine[1]

[1]*National Oceanic and Atmospheric Administration, Alaska Fisheries Science Center, National Marine Fisheries Service, 7600 Sand Point Way NE Seattle, WA 98115, USA*
[2]*Kongsberg Maritime AS, Strandpromenaden 50, P.O. Box 111, Horten 3191, Norway*

**Corresponding author: tel: +1-206-526-4789; e-mail: alex.derobertis@noaa.gov*

[†]These authors contributed equally to this work.

De Robertis, A., Bassett, C., Andersen, L. N., Wangen, I., Furnish, S., and Levine, M. Amplifier linearity accounts for discrepancies in echo-integration measurements from two widely used echosounders. – ICES Journal of Marine Science, 76: 1882–1892.

Received 21 November 2018; revised 31 January 2019; accepted 24 February 2019; advance access publication 8 April 2019.

The Simrad EK60 echosounder is widely used in acoustic-trawl surveys. It has recently been replaced by the EK80, which can be configured to operate in a manner similar to the EK60. To examine whether EK80s can be substituted for EK60s, the echosounders were configured to alternate transmissions from common transducers at four frequencies during three acoustic-trawl surveys. Significant differences between echo-integration measurements of fish were observed at 18, 38, and 70 kHz. EK80 measurements were 3–12% lower than those from EK60. At 120 kHz EK80/EK60 ratios were less than, but not statistically different from one. The EK80/EK60 discrepancy increased with range. The observed discrepancies were identified to be related to slight over-amplification of low-power signals (<-90 dB re 1 W) by EK60. EK80 amplified signals linearly over a wider range of measured powers. After accounting for over-amplification of weak signals by the EK60, the range dependence was removed and both echosounders produced equivalent results. The impact of over-amplification by the EK60 will be relatively small for surveys of strong scatters (fishes with swimbladders) at short ranges, but has the potential to be greater for surveys of weak scatterers and/or long observation ranges.

Keywords: acoustic survey, echo-integration, echosounder linearity, EK60, EK80, intercomparison.

Introduction

Acoustic-trawl surveys are widely used to aid in fisheries management. During these surveys, abundance is derived from echo-integration measurements made with calibrated echosounders and size and species composition from trawl samples (Simmonds and MacLennan, 2005). A primary goal of these surveys is to determine changes in abundance indices over time (National Research Council, 1998; Stenevik *et al.*, 2015), which requires the application of consistent methodology. Many acoustic-trawl surveys worldwide are, or have been, conducted with Simrad EK60 echosounders (Boyra *et al.*, 2013; Fielding *et al.*, 2014; Stenevik *et al.*, 2015), which are no longer commercially available (Demer *et al.*, 2017). These surveys either are, or will ultimately need to be, conducted with other instruments, and it is prudent to evaluate the performance of these alternatives relative to the EK60, so that the potential impact of changes in instrumentation on abundance surveys can be quantified.

The EK80 echosounder, the successor to the EK60, is capable of producing and processing broadband signals, which offer many potential benefits and have been an area of substantial

recent interest (Bassett *et al.*, 2017; Demer *et al.*, 2017; Lavery *et al.*, 2017). However, the EK80 was also designed to operate with single-frequency, continuous wave (CW) signals similar to those of the EK60 so that it can be used to continue acoustic-trawl time series. In principle, after appropriate calibration (Demer *et al.*, 2015), EK60 and EK80 systems operated in CW mode will produce equivalent survey results. The backscatter measurements underlying acoustic-trawl surveys depend on a complex chain of hardware and software, and it is helpful to compare the results of both instruments operated under realistic conditions. It is important to investigate whether any biases could be introduced into survey abundance indices used for fisheries management when survey methods are changed (Ona *et al.*, 2007; De Robertis and Wilson, 2011; Miller, 2013; Moriarty *et al.*, 2018), and substituting echosounders is no different.

Macaulay *et al.* (2018) compared EK60 and EK80 echosounders configured to alternate transmissions, and found that the echosounders produced echo-integration measurements within 0.6 dB (15%) at 38 kHz, which is a relatively large discrepancy (e.g. calibration precision is ∼±5% at 38 kHz; Foote *et al.*, 1987; Demer *et al.*, 2015). They observed range and power-dependent trends in the EK60/EK80 ratio, which were attributed to differences in the noise floor, but there are indications of smaller unexplained discrepancies in regions dominated by scattering from fish (see Figures 5–7 in Macaulay *et al.*, 2018). Thus, it remains unclear whether there are systematic differences between these instruments, and whether transitioning surveys from EK60 to EK80 instruments will result in negligible changes to survey abundance time series.

The aim of this study is to determine whether EK60 and EK80 instruments produce echo-integration measurements of fish that are comparable such that one might replace one with the other; that is, to test the hypothesis that $s_{A,\ EK80} = s_{A,\ EK60}$, where s_A is the nautical area backscattering coefficient. This term is an areal unit of integrated acoustic backscatter ($m^2\ nmi^{-2}$) widely used in fisheries acoustics, which is proportional to fish abundance (MacLennan *et al.*, 2002). We alternated pings from EK60 and EK80 electronics on the same transducers using a multiplexer device during three winter surveys of pre-spawning walleye pollock (*Gadus chalcogrammus*) in Alaska. The question being addressed is whether the two instruments measure the same mean backscattering coefficients over the long term (e.g. an entire survey), which is the most relevant metric for understanding whether surveys conducted with EK60 and EK80 instruments will produce equivalent results. The data from EK60 and EK80 echosounders were processed independently using standard methods to replicate a scenario in which the survey was conducted with either echosounder. The echosounders were calibrated on six occasions using the same methodology to quantify the uncertainties in the observed s_A attributable to calibration. Application of this calibration to field measurements, which are often much weaker signals than those from the calibration sphere, rests on the assumption that the echosounder has a linear response over the range of signals integrated. Although echosounder linearity has been measured in the past (Foote *et al.*, 1987) in current practice, the linearity of the echosounder is often unverified and the echosounder is assumed to be linear (Demer *et al.*, 2015). In other words, in many survey applications, a calibration derived from high-power measurements is assumed to be applicable to lower power signals. We characterized the linearity of EK60 and EK80 echosounders to investigate whether differences in how signals are amplified could explain differences between the instruments.

Methods

Study area

Echo-integration data from Simrad EK60 and EK80 echosounders were compared from three acoustic-trawl surveys of pre-spawning walleye pollock conducted in winter 2018 (Figure 1). Measurements were made along survey transects following established practice (McKelvey and Lauffenberger, 2017; Stienessen *et al.*, 2017) in the vicinity of the Shumagin Islands (7–12 February), Bogoslof Island region (3–7 March), and Shelikof Strait (15–22 March). Walleye pollock accounts for the majority of acoustic scattering during these surveys: in 2018, pollock accounted for 97.4% of trawl catch by weight in the Shumagin Islands, 98.5% in Bogoslof, and 97.6% in Shelikof Strait. These areas differ substantially in terms of pollock abundance and depth distribution. Briefly, pollock were relatively shallow and least abundant in the Shumagin Islands (Figure 2a); at intermediate densities at a variety of depths, including shallow in the water column (i.e. <75 m) in the Shelikof Strait area (Figure 2c); and deeply distributed at high densities in the Bogoslof survey (Figure 2e). The received electrical power of the signals (dB re 1 W, see Lunde and Korneliussen, 2016) varied over a wide range (Figure 2b, d, and f). Most of the echoes from fish were well below the power of the signals used for calibration (−53 to −75 dB re 1 W depending on frequency, see below).

Data collection

Paired EK60 and EK80 data sets were collected with the NOAA ship *Oscar Dyson* using a five-frequency (18, 38, 70, 120, and 200 kHz) system with transducers (Simrad model ES18, ES38B, ES70-7C, ES120-7C, ES200-7C) mounted on a retractable centreboard at a depth of 9.15 m. The EK60 and EK80 echosounders were configured to alternately collect pings on the same transducers during surveys conducted at a ship speed of 6 m s^{-1}. This was accomplished by means of a multiplexer and triggering system (Jech *et al.*, 2005; Macaulay *et al.*, 2018), which alternately connected the transducers to the EK60 and EK80 electronics and triggered data collection. Computer clocks were synchronized to a timeserver every 15 min, and the then-current software versions (EK80 v 1.11.1, and ER60 2.4.3) were used to collect echosounder data. The 200 kHz echosounders were too noisy to provide high signal-to-noise data at the depths where most of the fish were present (at >100 m, background noise was above the −70 dB re 1 m^{-1} integration threshold used in these surveys) and 200 kHz data were excluded from the analysis.

Each echosounder was operated by transmitting on all frequency channels simultaneously with a 1.024 ms pulse duration using the power settings recommended by Korneliussen *et al.* (2008). The EK80s were configured to produce CW signals with "fast" ramping applied (Demer *et al.*, 2017), which is the pulse configuration that most closely replicates the EK60 transmit pulses. We timed the interval between successive pings such that 2.2 times the time required to sample to the maximum bottom depth elapsed between pings. This interval was sufficient to eliminate above-threshold backscatter from the bottom echo from the previously transmitted ping (Renfree and Demer, 2016) at all frequencies. We also included a 100 ms delay before switching the transducers with the multiplexer and triggering the electronics to

transmit a ping. In the case of the Shumagin Islands, alternating pings were collected on EK80 and EK60 echosounders to 250 m at an interval of 0.85 s between EK60 and EK80 pings, in Bogoslof data were collected to 1000 m at an interval of 3.15 s, and in Shelikof data were collected to 300 m at a ping rate of 1.25 s. At the seaward end of transects in Bogoslof where bottom depths exceeded 1200 m, the EK80 was turned off to avoid further reductions in the EK60 ping rate during the survey.

Echosounder calibration

The on-axis standard sphere calibration technique (Demer *et al.*, 2015) was used to estimate the gain applied in echo integration (i.e. S_v gain, or the gain + s_A correction parameters). Calibrations were conducted at a range of ~20.5 m on six occasions between 27 January 2018 and 13 March 2018 with the EK80/EK60 multiplexing system in operation. A 64 mm copper sphere was used at 18 kHz, and a 38.1 mm tungsten-carbide sphere was used at the other frequencies. The measured power of the on-axis sphere echo was −53/−68/−68/−75 dB re 1 W at 18/38/70/120 kHz. A conductivity temperature and depth (CTD) cast was used compute sound speed and absorption coefficients at the calibration site. Calibration data from the EK60 and EK80 were processed in an equivalent fashion with the software used to post-process the survey data (Echoview 8.0.104).

During each calibration event, two replicate gain estimates were made except in one case where a single measurement was made, and another in which five replicates were conducted. The replicate measurements made during a single calibration event were transformed to linear units and averaged. The resulting calibration events ($n = 6$) were averaged in a similar fashion and used to estimate the average S_v gain ($\overline{G}$) used in post-processing. Calibration precision was estimated using a bootstrap approach (Efron and Tibshirani, 1991) with 5000 iterations: for each iteration, $n = 6$ calibration events were drawn with replacement and an estimate of gain was computed by averaging these events in linear units. The impact of applying this gain to compute the EK80/EK60 integration ratio [see Equation (2)] compared to the gain used for post-processing was estimated according to

$$g' = \frac{10^{\left[2\left(G_{\text{boot,EK80}} - \overline{G_{\text{,EK80}}}\right)/10\right]}}{10^{\left[2\left(G_{\text{boot,EK60}} - \overline{G_{\text{,EK60}}}\right)/10\right]}}, \quad (1)$$

where g' is the linear correction factor, $\overline{G}$ is the average S_v gain [dB] used in post processing, and G_{boot} is the S_v gain value [dB] of the bootstrapped sample. As with g', other variables defined with a prime symbol represent bootstrap samples. The 95% confidence intervals (*CI*s) representing the uncertainty introduced by calibration on the EK80/EK60 ratio were estimated by finding the 2.5 and 97.5 percentiles of the distribution of g'.

Data processing

Data along the survey transects were used for further analysis. Post-processing of the EK60 and EK80 data was conducted in an equivalent fashion using Echoview software. The mean S_v gain from the calibrations ($\overline{G}$) was applied. Otherwise, identical parameters influencing echo-integration values including the equivalent beam angle, absorption coefficients, and sound speed were applied to both systems. The rationale for this is that even if these parameters are inaccurate, they bias the backscatter

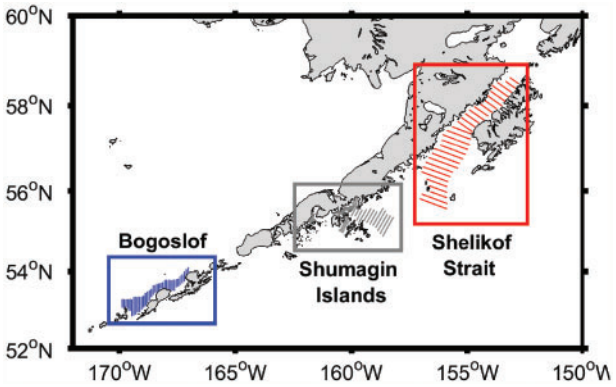

Figure 1. Map of the three survey areas showing transects where the EK80 and EK60 echosounders were compared.

estimated from the EK60 and EK80 echosounders in the same way, and will not affect the EK80/EK60 integration ratio.

Water column signals were isolated by editing a bottom exclusion line 3 m above a 5-frequency blended sounder-detected bottom computed with EK60 data (Jones *et al.*, 2011) as needed to exclude signals from the seafloor. A surface exclusion line at 18 m depth was edited to remove the nearfield and backscatter from bubbles swept under the transducer. The EK60 and EK80 data were visually reviewed to identify noise spikes or suspect near-bottom echoes, which were removed if present. The acoustic data were echo integrated into 5 min by 10 m deep bins using a −70 dB re 1 m^{-1} integration threshold to produce estimates of the nautical area scattering coefficient. Data aggregated at the transect level were also analysed, but are not presented as the results were similar.

To ensure that noise was not integrated into the s_A values, conservative depth limits were established for each frequency such that measurements above the integration threshold were driven by biological scattering rather than noise. These integration limits were 800, 700, 400, 120 m for the 18, 38, 70, and 120 kHz channels, respectively. The measurements considered were made at high signal-to-noise ratios: measurements with echosounder in passive mode (i.e. with the transmitter disabled) indicated that the −70 dB re 1 m^{-1} integration threshold was 11–32 dB greater than the noise floor (depending on frequency) of either instrument at the maximum range included in the analysis. In the Bogoslof survey, where fish were deeply distributed (Figure 2e and f), only the 18 and 38 kHz channels were post-processed. Data were exported and visualized in a series of diagnostic plots designed to identify potential outliers (e.g. maximum S_v in a given cell, outliers detected at a single frequency). In cases where outliers were detected, the data were re-examined and manually edited, if required, to exclude artefacts (e.g. noise spikes or bottom integrations).

Statistical analysis

The EK80/EK60 integration ratio r_i, defined as

$$r_i = \frac{s_{\text{A, EK80},i}}{s_{\text{A, EK60},i}}, \quad (2)$$

was estimated for each 5-min elementary distance sampling unit (EDSU, Simmonds and MacLennan, 2005), where s_A represents the nautical area scattering coefficient computed over the water column and i is an index corresponding to the EDSU. We

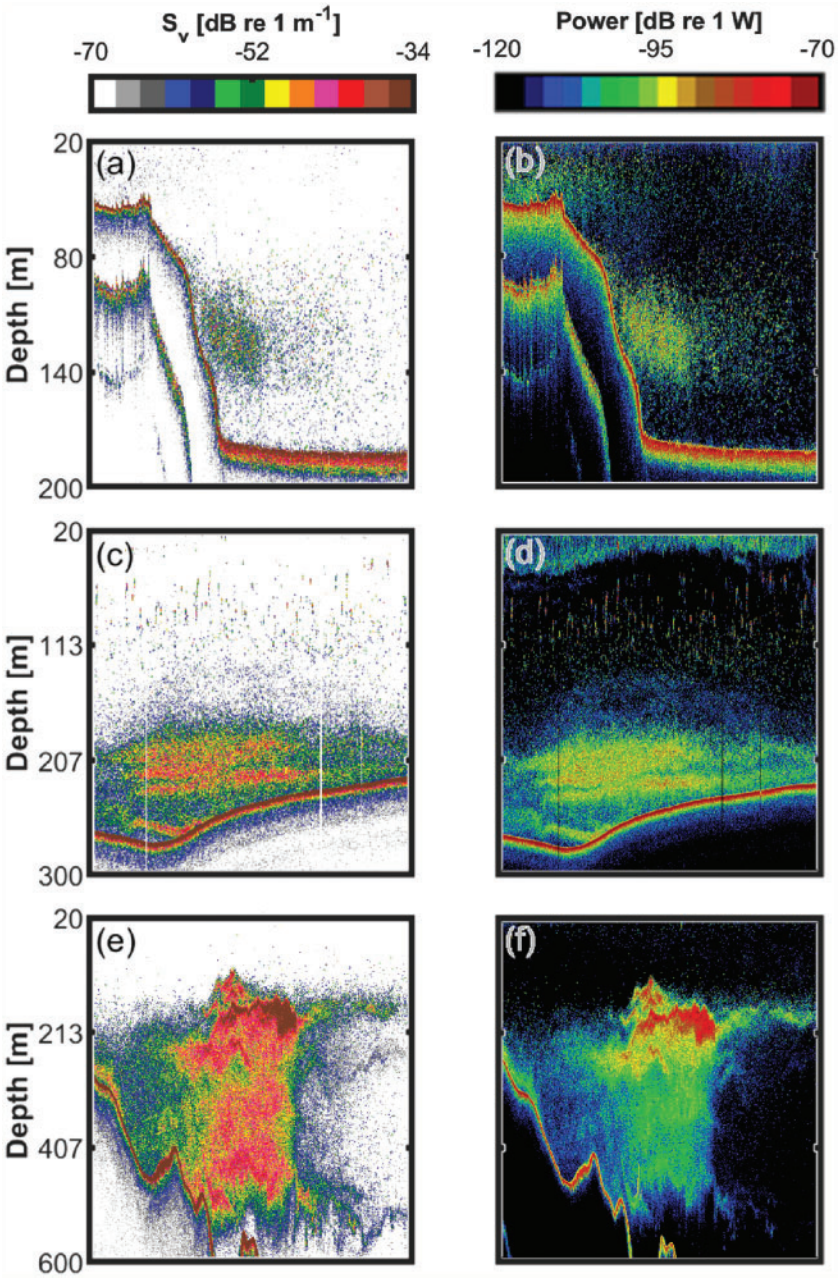

Figure 2. Echograms (38 kHz EK60) showing S_v (first column) for high-density pollock aggregations along with received power (second column). (a and b) Shumagin Islands area, where the mean fish depth was 124 m (95% of EDSUs 67–169 m). (c and d) Shelikof Strait, where the mean fish depth was 150 m (95% of EDSUs 53–237 m). (e and f) Bogoslof Island area, where the mean fish depth was 336 m (95% of EDSUs 210–445 m). Calculation of fish depth follows Equation (4) of De Robertis and Wilson (2011), and was computed for EDSUs with s_A >100 m^2 nmi^{-2}.

excluded partial EDSUs (i.e. those where <95% was on a survey transect), and cases where backscatter in either instrument was low (s_A <100 m^2 nmi^{-2}) as preliminary analysis indicated that r_i was more variable where fish were scarce. The mean EK80/EK60 integration ratio was computed as

$$\hat{r} = n^{-1} \cdot \sum_n r_i, \quad (3)$$

where n corresponds to the number of EDSUs.

The 95% *CI*s of $\hat{r}$ were estimated via bootstrapping. To account for spatial variability, a bootstrap sample was generated by drawing n observations of $s_{A,j}$, where j is drawn with replacement from the EDSU indices (i) of the original data set,

$$r'_j = \frac{s_{A,\,EK80,j}}{s_{A,\,EK60,j}}. \quad (4)$$

The mean ratio for the EDSU bootstrap sample is computed as per Equation (3),

$$\hat{r}' = n^{-1} \cdot \sum_{n} r'_j. \quad (5)$$

Finally, to account for the effects of calibration uncertainty, these estimates are multiplied by a randomly drawn calibration factor [g' see Equation (1)],

$$\hat{r}'_{\text{tot}} = \hat{r}' \cdot g'. \quad (6)$$

The mean and 95% *CI*s of the EK80/EK60 integration ratio were estimated by finding the mean and 2.5 and 97.5 percentiles from the 5000 bootstrap realizations of $\hat{r}'_{\text{tot}}$. In general, results are presented in detail for the 38 kHz data, as this is the primary frequency used in these and many other acoustic surveys of fish (Furusawa, 1991). Results for the other frequencies are summarized or given as Supplementary Material.

The potential for range-dependence in the EK80/EK60 ratio was explored by computing $\hat{r}'_{\text{tot}}$ for 10 m layers (i.e. rather than vertically integrated results as described above) for all data where $s_A > 10$ m^2 nmi^{-2} in both echosounders. Bootstrap *CI*s of the mean were estimated for each range bin as described above. To increase the amount of data in shallow water for these calculations an additional 41 five-min EDSUs where fish were located at <50 m were selected from periods when the vessel was transiting. These additional data were used only to evaluate range dependence of the EK80/EK60 integration ratio.

Measurement of echosounder amplification

The amplifier linearity of the EK60 and EK80 echosounders was measured using a test system designed to measure EK60 and EK80 using the same methodology. The approach is similar to that described in Foote *et al.* (1987). A common mode choke (Shaffner RN112-1, 2/02) used as a coupling transformer creating a differential signal from a single-ended CW pulse at the echosounder's operating frequency provided by a signal generator (Agilent 33500B). The signals were stepped from 0.1 to 9.9 V in 0.1 V steps. Each signal was passed through one of four passive attenuators and measured at the receive terminals of the EK60 or EK80. Received power levels were recorded by EK80 software with no time-varying gain applied. The use of the EK80 software ensures that the digital filters are applied to the received signals. The four attenuator circuits reduced the input voltages by ~1/330 000, 1/10 700, 1/1000, and 1/16 (EK60) or 1/25 (EK80). The difference in the lowest attenuator circuits for the EK60 and EK80 was driven by the different impedances of the EK60 and EK80 transceivers. Given the voltages and the observed noise levels, amplification could be measured from −40 to −130 dB re 1 W, which covers the dynamic range of the measurements included above the echo-integration threshold used in this study. A Keysight 34410A digital multimeter was used to verify the output of the signal generator. This multimeter could also be used to measure the input voltage to the transceiver from the two smallest attenuators.

For each measurement, the input power was calculated based on the voltage setting of the signal generator and the attenuator used ($P_{\text{in}} = V^2/R$, where V is the attenuated voltage and R is the nominal impedance of the transceiver). The exact values of the attenuators are unknown. However, the attenuators were designed such that the recorded power outputs from the different stages would overlap. Therefore, the data were manually shifted by a constant such that measurements from one attenuator to the next overlapped/transitioned with minimal discontinuities under the assumption that the amplifier response is continuous. We normalized the measurements such that the ratio between the expected and measured power expressed in linear units (Δp) was 1 at the power at which the calibration measurements were made. The resulting data were smoothed with a three-point running mean (except near the edges of the measurement range where the number of points was reduced to maintain a symmetrical averaging window) and then fit with a piecewise cubic Hermite spline fit (Supplementary Figure S1). Measurements were made on the specific EK60 and EK80 echosounders used in this study and other EK60 and EK80 echosounders. Measurements were made at 18 kHz (one EK60; one EK80), 38 kHz (four EK60s; eight EK80s), 70 kHz (three EK60s; three EK80s), and 120 kHz (one EK60; two EK80s). The measurements on the specific EK60 echosounders used in this study were repeated (four times at 38 kHz, two times for other frequencies) and averaged, while a single measurement was made for the other instruments. The repeated measurements of EK60 linearity agreed to within 1–2% across the range of measured powers.

Correction for amplifier linearity

A correction accounting for the effect of measured amplifier linearity on backscatter measurements was implemented. The effect of the linearity measurements on the EK80/EK60 ratio was estimated as $\text{corr}_{,P_{\text{in}}} = \Delta p_{\text{EK80},P_{\text{in}}} / \Delta p_{\text{EK60},P_{\text{in}}}$. The results for the specific EK60s and EK80s used on the *Oscar Dyson* were used to develop the correction for each frequency. A set of EK60 files with an adjustment for the combined effect of EK60 and EK80 linearity on the EK80/EK60 integration ratio was written by correcting each EK60 received power sample [i.e. $P_{\text{corr}} = P_{\text{meas}} + 10\log_{10}(\text{corr}_{,P_{\text{in}}})$] using a Matlab script based on the Echolab toolkit (Towler, 2017). The EK80/EK60 ratios were re-computed from the corrected files to assess whether the results change if the measurements of amplifier linearity for these instruments are taken into account.

Results

The estimates of integration gain from the six calibration events were similar. In the case of 38 kHz, the 95% intervals of g' indicated that the expected impact of calibration uncertainty on the EK80/EK60 ratio, which relies on the mean gain estimated from six calibrations, ranged from 0.98 to 1.03. That is, at 38 kHz, discrepancies of >3% in the EK80/EK60 ratio cannot be attributed to sampling uncertainty and calibration precision alone, and are likely to be related to other processes influencing the measurements. Overall, calibration uncertainty increased with frequency (Figure 3), introducing an uncertainty of ~2% on the EK80/EK60 integration ratio at 18 kHz, 3% at 38 kHz, 7% at 70 kHz, and 9% at 120 kHz (Figure 3).

Backscatter observed with the EK80 was consistently lower than that observed by the EK60, at both the scale of 5-min EDSUs, and when averaged over the survey area. For example, at the EDSU scale, the 38 kHz the EK60 s_A measurements exceeded those from EK80 in 69.4% of the measurements (Figure 4). The survey-average backscatter (i.e. integrated over all depths and EDSU's) observed with the EK80 was consistently lower (2–7%) than that with EK60 for all surveys and frequencies (Table 1). Survey-average ratios for all 10 comparisons were <1, which

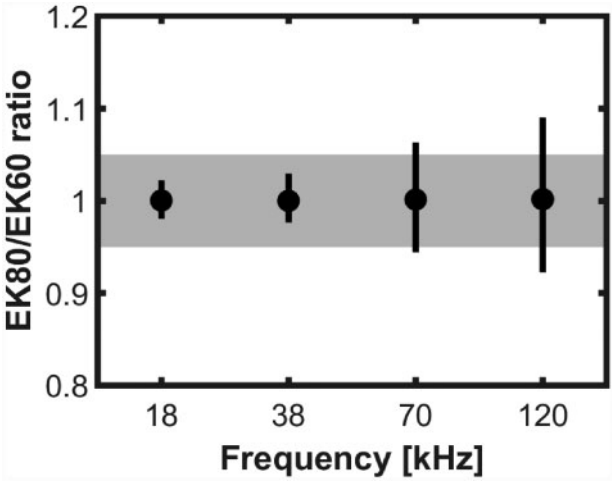

Figure 3. Mean and 95% *CI*s showing the impact of calibration uncertainty [g', Equation (1)] on the EK80/EK60 echo-integration ratio as a function of frequency. The grey band demarcates ±5%. Higher precision of calibrations at the lower frequencies results in narrower 95% *CI*s.

is unlikely if there was no difference between instruments [$p <$ 0.001 (binomial test) if there is a 50% chance of observing a ratio <1].

The EK80/EK60 integration ratios [$\hat{r}'_{\text{tot}}$, see Equation (3)], which estimate a similar quantity and also provide an estimate of the variance, indicate that backscatter observations from the EK80 echosounder were consistently lower than backscatter measurements from a similarly calibrated and configured EK60. The bootstrap estimates of sampling variability indicate that for all data combined, the EK80/EK60 integration ratio at 38 kHz was 0.94 (Figure 5a, 95% *CI* 0.93–0.94), and including the calibration uncertainty in the error budget [Equation (6)] did not cause the *CI*s to overlap with 1 (Figure 5b, 95% *CI*, 0.91–0.96). This trend was evident at other frequencies, with overlapping confidence bounds for the EK80/EK60 ratio across frequency (Figure 6). However, the *CI*s increased with frequency due to a shorter effective range, lower sample sizes (Table 1), and higher calibration uncertainty at higher frequencies (Figure 3). At 18, 38, and 70 kHz $s_{A,EK80}$ was 3–12% lower than $s_{A,EK60}$, and the 95% *CI*s for excluded one in all cases but Shelikof Strait at 38 kHz (Figure 6). At 120 kHz the EK80 was 4–8% lower than EK60, but the 95% *CI*s for the EK80/EK60 integration ratio included one, meaning that when calibration and spatial effects are accounted for, the results from EK80 and EK60 were not significantly different. These results were not sensitive to the $s_A > 100$ m^2 nmi^{-2} criterion: repeating the analysis shown in Figure 6 with a threshold of $s_A > 1$ m^2 nmi^2 resulted in similar ratios (average difference of 1.2%, range: 0.1–4.4%). However, uncertainty generally increased as the inclusion of more variable low-backscatter observations (Figure 4) counteracted the effect of increased sample sizes [95% *CI*'s increased by an average of 34.6% (range: −5.4 to 65.4%)].

The ratios differed among survey areas, with lower EK80/EK60 ratios in Bogoslof where the biomass is dominated by deeply distributed pollock (Figure 2e). In contrast, the ratios were closer to one in the Shumagin Islands and Shelikof Strait areas which were dominated by shallower backscatter (Figure 2a and c). The EK80/EK60 ratio exhibited range dependence, with ratios variable but not significantly different from one at <∼100 m, and decreasing to ∼0.8 at ranges of 700 m (see Figure 7 for 38 kHz, Supplementary Figure S2 for other frequencies).

Measurement of echosounder linearity indicated that the EK60 slightly over-amplified low-power signals. The EK60 was linear (to within 3%) for powers of −40 to −90 dB re 1 W, but increasingly over-amplified weak signals (Figure 8a and Supplementary Figures S3 and S4). At low powers (< −110 dB re 1 W), the measurements are more variable both within and across units (Supplementary Figures S2 and S3) likely due to the influence of electromagnetic interference and the inherent thermal noise of the system. In contrast, all EK80s tested were linear to ∼5% from −40 to −130 dB re 1 W. Measurement of a single EK80 at multiple frequencies produced similar results (Supplementary Figure S5).

Measurement of echosounder linearity indicates that over-amplification of low-power signals by EK60 will result in lower EK80/EK60 ratios when the instruments are calibrated at high power. This will introduce range-dependence, as spreading and absorption losses lead to lower-power signals. After accounting for the effect of the measured amplifier response on the EK80/EK60 ratio (Figure 8a), the EDSU-level ratios were close to 1 (compare Figures 6 and 8b). With only one exception (the lower bound for 18 kHz in Bogoslof was 1.01) the *CI*s were not significantly different from a ratio of 1. However, these *CI*s are overly narrow as they do not incorporate uncertainties in the linearity correction, which if included, would likely indicate that the discrepancy in Bogoslof at 18 kHz is not significant. The survey-average backscatter ratio, which was consistently <1 before correction (Table 1), was also close to 1 after correcting for instrument linearity (Table 2). The range-dependence in the EK80/EK60 ratio was no longer evident after accounting for echosounder linearity (see Figure 8c for 38 kHz, Supplementary Figure S6 for other frequencies).

Discussion

The primary finding of this study is that echo-integration measurements from EK80 instruments are consistently lower than those from EK60 instruments across the range of frequencies commonly used in fisheries acoustics. This discrepancy was range-dependent, which suggested that the amplification of one or both instruments might not be completely linear as is required when applying calibration measurements of gain to measurements at different power levels than those at which the calibration was conducted (Foote *et al.*, 1987; Demer *et al.*, 2015). The range dependence caused us to investigate the linearity of the instruments involved, and ultimately attribute the discrepancy in the EK80/EK60 integration ratio to over-amplification of weak signals (< −90 dB re 1 W) by the EK60. The EK80 is linear over a broad range of powers. In our application, calibration occurred at powers higher than the signals from most fish aggregations, and this resulted in the EK60 over-estimating backscatter from the biological targets.

Echo-integration measurements made with EK80 were ∼3 to 12% lower than those from EK60, depending on frequency, for the three surveys in this study. Based on the *CI*s, the differences observed at 18/38/70 kHz are outside those attributable to sampling variability and calibration uncertainty alone, which indicates a systematic difference between the instruments. At 120 kHz, average echo-integration measurements from the EK80 in this study were lower than those from the EK60, but the

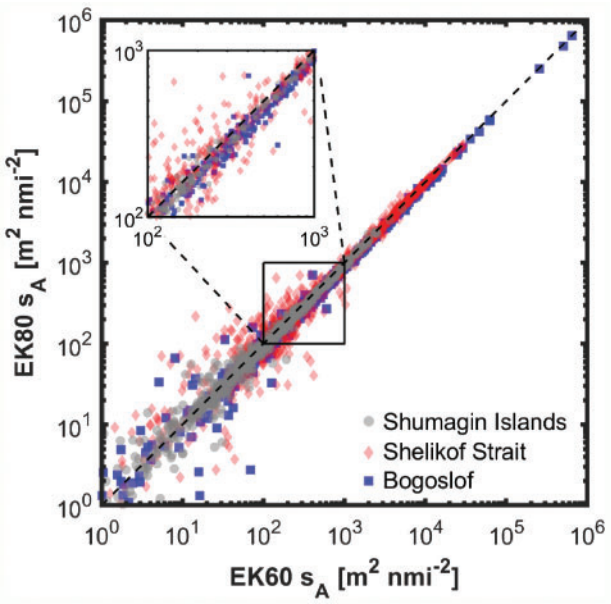

Figure 4. EK60 s_A vs. EK80 s_A for five-min EDSUs from the 38 kHz channels. The inset is an expanded view showing that many of the individual points are below the 1:1 line.

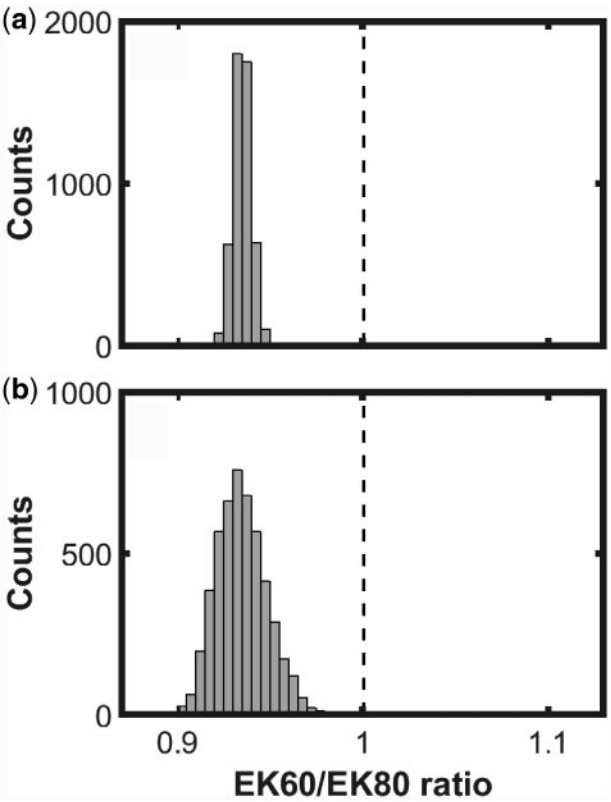

Figure 5. (a) Bootstrap estimates of spatial variability on 38 kHz EK80/EK60 ratios [Equation (5)] for samples combined from all three surveys, where s_A >100 m^2 nmi^2 (n = 1236 EDSUs). (b) Bootstrap estimates combining the effects of spatial sampling (a) and calibration uncertainty on the EK80/EK60 echo-integration ratios [Equation (6)].

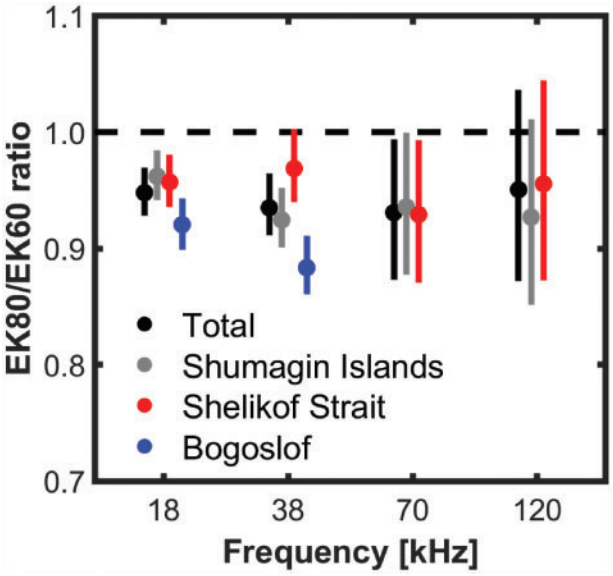

Figure 6. Mean EK80/EK60 integration ratios and 95% *CI*s including spatial and calibration uncertainty [Equation (6)] for all observations combined and individual survey areas. The survey areas are listed in order of fish depth. The dotted line indicates the expectation for no difference between the instruments. The differences among surveys are attributed primarily to the strength of the received signal, with ratios decreasing when low-power signals from deep or sparse fish are included. Sample sizes are given in Table 1.

differences were not statistically significant. This is likely attributable to higher uncertainty due to lower calibration precision, and smaller data sets and more variable fish distributions given the 120 m depth limit imposed at 120 kHz. Survey-wide average backscatter from EK80 was 2–7% lower than from EK60. Discrepancies for survey-wide average backscatter were noticeably smaller than the EDSU level discrepancies in Bogoslof. This is because areas with high fish densities (and high amplitudes) contribute disproportionately to survey-averaged backscatter (Macaulay *et al.*, 2018). In Bogoslof, dense pollock aggregations at moderate depths resulted in high-amplitude measurements (Figure 2e and f) where both the EK60 and EK80 are linear relative to the power at which they were calibrated (Figure 8a). Overall, the differences reported here are on the order of those reported in a similar study (Macaulay *et al.*, 2018) where EK80/EK60 integration ratios were reported to agree within 0.6 dB or 15%. One key difference between the results reported here and those of Macaulay *et al.* (2018) is that we attribute these discrepancies to systematic differences between EK60 and EK80 echosounders.

There is evidence for range-dependence such that the EK80 produces lower echo-integration values than EK60 for fish at longer range. In instances where fish were shallower than 100 m measurements from EK60 and EK80 were more similar. Where pollock were more deeply distributed (e.g. Bogoslof), the average EK80/EK60 integration ratio was lower. This range-dependence is due to slight over-amplification of low-power signals by the EK60 echosounder, which will bias abundance estimates as it violates the assumptions inherent in echo integration (Foote, 1983). Given that the received signals are strongly attenuated with range due to spreading and absorption while calibration occurs at high

Table 1. Backscatter ratio (EK80/EK60) observed during the three surveys.

Frequency [kHz]	Shumagin Islands, 586 EDSUs	Shelikof Strait, 863 EDSUs	Bogoslof, 559 EDSUs
18	0.96 (265)	0.94 (632)	0.98 (350)
38	0.93 (235)	0.96 (636)	0.94 (365)
70	0.95 (220)	0.94 (632)	n/a
120	0.93 (77)	0.95 (435)	n/a

Entries represent the ratio of the EK80/EK60 integral computed over the entire survey (i.e. $\sum_i s_{A,EK80,i} / \sum_i s_{A,EK60,i}$, where s_A represents the nautical area scattering coefficient and *i* represents the EDSU). The total number of EDSUs (which are used in this calculation) is given in the top row. The sample size used in Equation (3) (number of 5-min EDSUs with $s_A > 100$ m^2 nmi^{-2} subject to depth limits) is given in parentheses for each entry. Frequencies that were not analysed in the Bogoslof survey are identified as n/a.

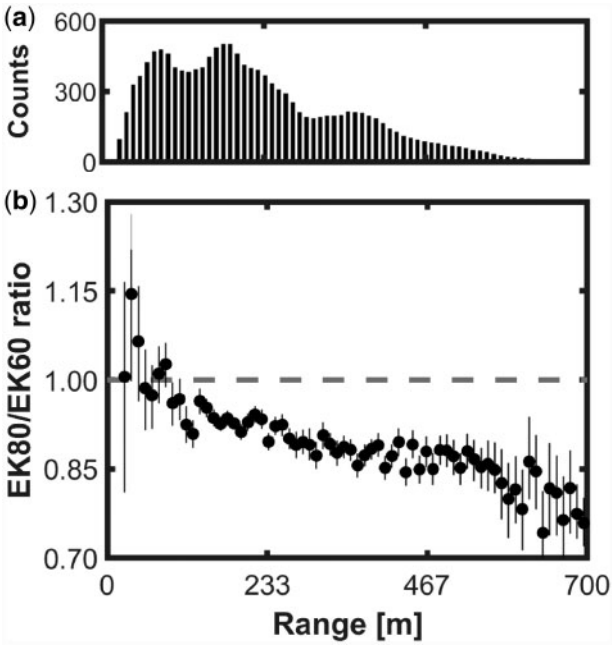

Figure 7. EK80/EK60 integration ratios at 38 kHz as a function of range (a) Number of valid measurements (i.e. those with $s_A > 10$ m^2 nmi^{-2} in a 5-min by 10-m cell) as a function of range. (b) Mean and 95% *CI* of the EK80/EK60 integration ratio [Equation (5)] as a function of range in 10 m range bins. The EK60/EK80 ratio is range dependent with values <1 at ranges >∼100 m. The elevated uncertainty at short ranges is driven by small sample size and higher spatial variability.

power, the calibrated gain may not be appropriate for lower-power measurements of fish at long ranges. At short ranges, measurements of fish backscatter from EK60 and EK80 will be equivalent, because both instruments are linear at powers <−90 dB re 1 W. Thus, the discrepancy between these instruments will depend on multiple factors including the linearity of the equipment used, the signals transmitted, the range and sphere used for calibration, range to aggregations dominating the backscatter, the density of the scatterers, and the acoustic scattering strength of the animals.

We designed the comparison to minimize potential biases in our experimental design. By using a multiplexer system, we were able to drive the same transducers on the EK80 and EK60 electronics. We cannot entirely rule out that the multiplexer affected the measurements, but did not observe any effects during initial testing and calibration with and without the multiplexer. Using the same transducer for both echosounders reduces uncertainties compared to using independent transducers. This includes uncertainties related to the volume sampled (i.e. the equivalent beam angle), which is not characterized by the standard sphere calibration method, and can be a major source of uncertainty in echo-integration measurements (Haris *et al.*, 2017). In addition, we applied the same environmental parameters (e.g. sound speeds, absorption coefficients) when processing both data sets. Any inaccuracies in these parameters result in equivalent biases for both echosounders, which will not affect the EK80/EK60 integration ratio. We applied the same calibration procedures and the same software to process the calibrations and echo-integration measurements from both systems. This may have led to better agreement between instruments than if echosounder specific protocols were used as there are small differences in how calibration is implemented in the EK60 and EK80 software (Macaulay *et al.*, 2018).

The use of numerous calibrations is key to investigating potentially significant differences between echosounder systems. Multiple calibrations of both systems allows for the effect of calibration uncertainties on the EK80/EK60 ratio to be quantified. Given that the ratios of the echo-integrated data for the survey are relatively close to one, the observed variability of the EK80/EK60 ratio for a single calibration is generally larger than the observed discrepancies (Supplementary Figure S7). Without multiple calibrations it would not be possible to define sufficiently narrow *CI*s to identify and further investigate differences in the echo-integrated values between the systems.

The discrepancies between EK80 and EK60 are also potentially attributable to either the echosounder hardware/software or the post-processing software used. Given that the EK80 is a new instrument, we conducted a series of tests to investigate whether the differences in the echo-integrated results could be attributed to the post-processing methods used for this instrument. For example, echo-integration measurements of an on-axis calibration sphere processed with Echoview and the EK80 calibration software were close (Echoview/EK80 ratio: 1.005 ± 0.006, $\overline{x} \pm SD$). We also found that ranges to a sphere moved through the beam were similar when processed with Echoview and EK80 calibration software (range discrepancy of 0.03 ± 0.03 m, $\overline{x} \pm SD$). One potential explanation for the observed range-dependence is that the attenuation or time-varying gain was accounted for improperly in post-processing. We ruled this out by confirming that the specified attenuation values were correctly applied to the EK60 and the EK80 data. In addition, we verified that volume backscattering was correctly being computed from received power for both instruments. Thus, although minor differences may remain, our conclusions are consistent with those of Macaulay *et al.*

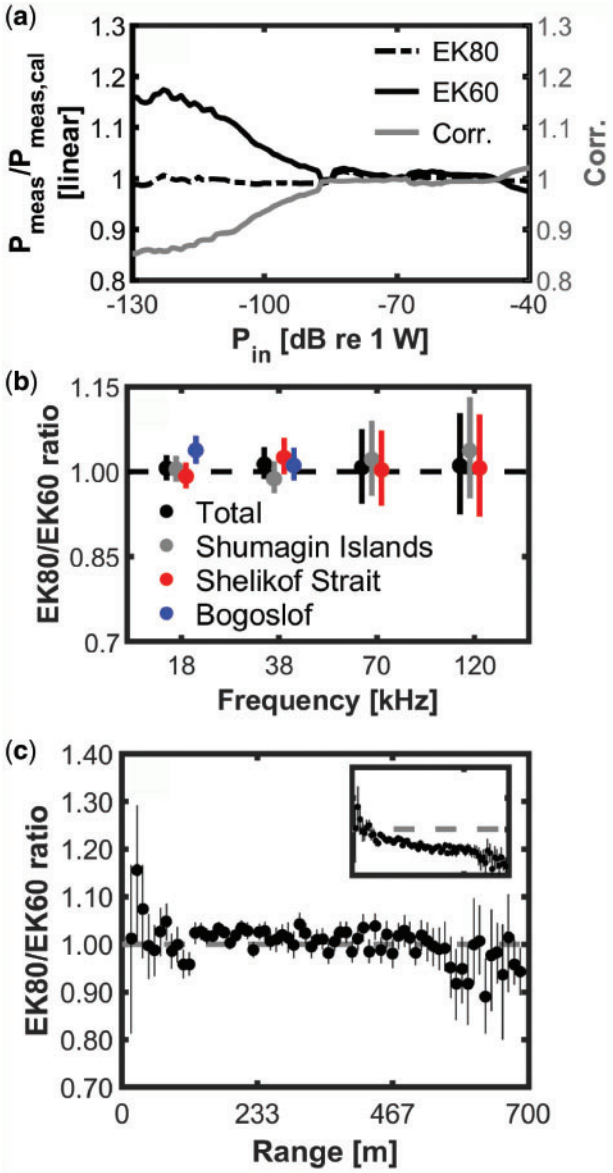

Figure 8. (a) Measurement of echosounder amplification at 38 kHz. The EK60 over-amplifies weak signals by up to ∼18%, while the EK80 is linear to within 3% over the depicted range. Corr refers to the correction applied to EK60 data to correct for the measured 38 kHz amplifier response on the EK80/EK60 ratio. (b) EK80/EK60 ratios are close to 1 after correcting for the EK80/EK60 amplification ratio. (c) EK80/EK60 ratio at 38 kHz as a function of range after correction for the amplifier ratio. The inset shows the results for the uncorrected data (i.e. Figure 7b) on the same scale for comparison.

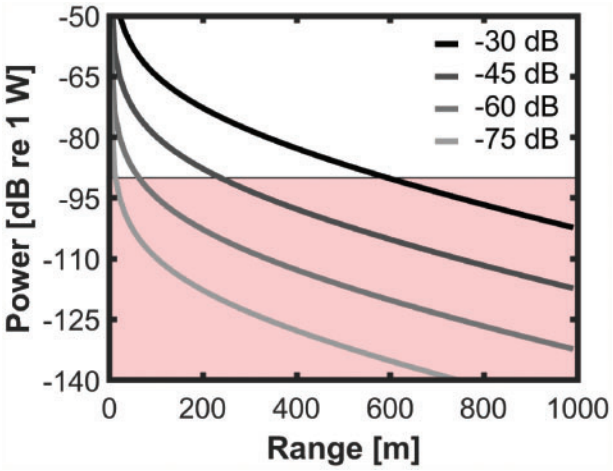

Figure 9. Approximate power as a function of range for a 38 kHz EK60 equipped with an ES38B transducer for a given level of volume scattering (S_v, dB re 1 m^{-1}). The shaded area denotes powers <90 dB re 1 W, where backscatter begins to be over-estimated by EK60 (see Figure 8a).

Table 2. EK80/EK60 backscatter ratio observed during the three surveys after correction for measured amplifier response.

Frequency [kHz]	Shumagin Islands	Shelikof strait	Bogoslof
18	0.99	0.97	1.02
38	0.98	1.02	1.01
70	1.02	1.03	n/a
120	1.04	0.99	n/a

This is the same as Table 1, but computed after applying the correction shown in Figure 8a.

(2018) that post-processing software packages are correctly computing volume backscatter. The small discrepancies we observed were insufficient to explain our observation of differences in echo-integration results from EK80 and EK60 echosounders.

In our study, five frequencies were transmitted simultaneously as is common practice with these instruments. However, the EK80 and EK60 operated in CW mode may have different receiver bandwidths (Demer *et al.*, 2017). Thus there is the potential for differences in cross-channel interference due to nonlinear acoustic propagation at high sound pressures (Tichy *et al.*, 2003; Demer *et al.*, 2017). This effect, where the response at a given frequency can be affected by harmonics caused by transmission at other frequencies is a potential mechanism for the observed range-dependence, as this additional signal is range-dependent (Tichy *et al.*, 2003), and calibrations at short ranges would not be applicable at longer ranges where the nonlinear effects are attenuated. Macaulay *et al.* (2018) suggest that crosstalk and subharmonic interference caused by simultaneously transmitting EK60 echosounders at several frequencies may have affected the EK80/EK60 ratio. However, comparison of calibration results conducted with all channels pinging synchronously and others with only one channel active at a time indicated that estimates of the maximum effects of potential cross-channel interference were too small to explain the observed range-dependent effects (Supplementary Figure S8). Thus, differential effects of crosstalk between channels cannot explain the observed range-dependent EK80/EK60 integration ratio.

Previous studies of echosounders used in acoustic-trawl surveys have primarily focused on short-range measurements under controlled conditions (Jech *et al.*, 2005; Demer *et al.*, 2017), in great part because such measurements are controlled and the quantities of interest can be precisely estimated. However, this does not capture all the conditions encountered in a survey (e.g. low-power signals), and it is thus valuable to complement these studies with field validations that evaluate system performance in

a wide range of realistic conditions. Because of the variability of field measurements, sample sizes must be large for the comparison to resolve small but meaningful differences. In addition, the observations must cover a wide range of conditions. In this study, without sufficient sampling across a wide depth range the power dependence in the EK80/EK60 ratio would have been less evident.

The discrepancies in the EK80/EK60 ratio identified in this study are associated with slight over-amplification of low-power signals relative to high-power signals by the EK60, which can be considered a calibration issue. Calibration measurements are made at high power to ensure high signal-to-noise measurements, but as in the surveys considered here, the resulting gains are often applied to low-power measurements. This assumption has long been recognized, but is often overlooked. Foote *et al.* (1987) discuss this assumption and discuss how to make electrical measurements to measure amplifier linearity and other aspects of echosounder performance. However, in current practice, echosounders used in fisheries acoustics are generally assumed to be linear but this is generally not verified. This work suggests that amplifier linearity should be considered explicitly when calibrating echosounders, and that further efforts are needed to develop practical methods to characterize the linearity of quantitative echosounders. One option is to characterize echosounder linearity in the laboratory (Foote *et al.*, 1987). Given that these measurements will be difficult for many users to make, manufacturers would ideally measure the amplifier response of each quantitative echosounder, or demonstrate the linearity of a particular model. Another approach may be to expand calibration to span the range of powers used to make field measurements. Calibrating over the useful dynamic range of modern echosounders using the standard sphere method is likely to be impractical as suspension tethers are likely to interfere with weak targets, and stronger targets would have to be deployed at very long ranges to calibrate at low power. Development of an inline attenuator to reduce the received signal from a standard calibration sphere may prove a practical solution.

In the context of the large dynamic range (>100 dB) of the instruments the over-amplification of weak signals by the EK60 reported here is rather slight. While the measurements suggest that low-power signals can be over-amplified by ∼20%, given that higher power-signals contribute disproportionately to estimates of biomass (e.g. compare Table 1 and Figure 6), this is likely to introduce only modest uncertainty in many acoustic surveys of strong acoustic scatters at short range (e.g. Figure 9). In surveys of fish with swimbladders at greater depths, average measurements from EK60 will be biased slightly high (3–12% in this study). For low-power signals from sparse, weakly scattering and/or deeply distributed organisms (Proud *et al.*, 2017), the differences will be larger.

Conclusions

Comparison of EK60 and EK80 echosounders configured to transmit single-frequency CW signals similar to those produced by the EK60 indicates that survey abundance estimates based on EK80s will be consistently lower than those from EK60 echosounders when low-power signals are measured. This discrepancy (up to 12% in the surveys considered here) is attributable to nonlinear amplification of low-power signals by EK60, which results in a range and density-dependent bias in echo-integration measurements. After correcting for the amplifier response of the two systems, the range dependence was removed and the echo-integrated results from the two echosounders showed good agreement. Thus, although calibrated EK60 and EK80 echosounders produce similar echo-integration measurements for high-power signals, measurements on lower power signals with EK60s will be biased high. The EK80 is linear to within ∼5% over the useful dynamic range, and represents an improvement over the EK60.

The magnitude of biases introduced by amplification will depend on the characteristics of the echosounder used, the received power of the observed signal relative to that at calibration, which are related to calibration practice and the depth distribution, abundance, and scattering strength of the organisms being surveyed (Figure 9). The consequences of echosounder linearity and methods for measurement of linearity have long been understood (Foote *et al.*, 1987), but the subject has received relatively little attention. The linearity of many quantitative instruments remains poorly characterized. Although the errors introduced by over-amplification of low-power signals by EK60 are relatively small relative to other sources of uncertainty in acoustic surveys (McClatchie and Coombs, 2005; Simmonds and MacLennan, 2005; Ona *et al.*, 2007; Williams *et al.*, 2011; Haris *et al.*, 2017), the linearity of this and other calibrated instruments can be characterized and, if needed, corrected for.

Acknowledgements

David Demer, Josiah Renfree, and members of NOAA's Advanced Survey Technologies group built the multiplexing system and lent us three EK80 transceivers. Dezhang Chu loaned two additional EK80s. Toby Jarvis and Geoff Matt verified the calculations performed by Echoview software. Chris Wilson initiated this work and members of the midwater assessment group at the Alaska Fisheries Science Center contributed to the field work.

Supplementary data

Supplementary material is available at the *ICESJMS* online version of the manuscript.

Funding

This work was supported by NOAA's Alaska Fisheries Science Center and NOAA's Office of Science and Technology, Advanced Sampling Technology Working Group. References to trade names do not imply endorsement by the National Marine Fisheries Service, NOAA.

References

Bassett, C., De Robertis, A., and Wilson, C. 2017. Broadband echosounder observations of frequency response during from fisheries surveys in the Gulf of Alaska. ICES Journal of Marine Science, 3: 1131–1142.

Boyra, G., Martinez, U., Cotano, U., Santos, M., Irigoien, X., and Uriarte, A. 2013. Acoustic surveys for juvenile anchovy in the Bay of Biscay: abundance estimate as an indicator of the next years recruitment and spatial distribution patterns. ICES Journal of Marine Science, 70: 1354–1368.

Demer, D. A., Andersen, L. N., Bassett, C., Berger, L., Chu, D., Condiotty, J., Cutter, G. R. *et al.* 2017. 2016 USA–Norway EK80 Workshop Report: evaluation of a wideband echosounder for fisheries and marine ecosystem science. ICES Cooperative Research Report, 336. 69 pp.

Demer, D. A., Berger, L., Bernasconi, M., Bethke, E., Boswell, K., Chu, D., and Domokos, R. 2015. Calibration of acoustic instruments. ICES Cooperative Research Report, 326. 130 pp.

De Robertis, A., and Wilson, C. D. 2011. Silent ships do not always encounter more fish (revisited): comparison of acoustic backscatter from walleye pollock recorded by a noise-reduced and a conventional research vessel in the eastern Bering Sea. ICES Journal of Marine Science, 68: 2229–2239.

Efron, B., and Tibshirani, R. 1991. Statistical data analysis in the computer age. Science, 253: 390–395.

Fielding, S., Watkins, J. L., Trathan, P. N., Enderlein, P., Waluda, C. M., Stowasser, G., Tarling, G. A. *et al.* 2014. Interannual variability in Antarctic krill (*Euphausia superba*) density at South Georgia, Southern Ocean: 1997–2013. ICES Journal of Marine Science, 71: 2578–2588.

Foote, K. G. 1983. Linearity of fisheries acoustics, with addition theorems. Journal of the Acoustical Society of America, 73: 1932–1940.

Foote, K. G., Knudsen, H. P., Vestnes, G., MacLennan, D. N., and Simmonds, E. J. 1987. Calibration of acoustic instruments for fish density estimation. ICES Cooperative Research Report, 144. 81 pp.

Furusawa, M. 1991. Designing quantitative echo sounders. Journal of the Acoustical Society of America, 90: 26–36.

Haris, K., Kloser, R., Ryan, T. E., and Malan, J. 2017. Deep-water calibration of echosounders used for biomass surveys and species identification. ICES Journal of Marine Science, 75: 1117–1130.

Jech, J. M., Foote, K. G., Chu, D., and Hufnagle, L. C. 2005. Comparing two 38-kHz scientific echosounders. ICES Journal of Marine Science, 62: 1168–1179.

Jones, D. T., De Robertis, A., and Willamson, N. J. 2011. Statistical combination of multifrequency sounder-detected bottom lines reduces bottom integrations. NOAA Technical Memorandum NMFS-AFSC-219. 13 pp.

Korneliussen, R. J., Diner, N., Ona, E., Berger, L., and Fernandes, P. G. 2008. Proposals for the collection of multifrequency acoustic data. ICES Journal of Marine Science, 65: 982–994.

Lavery, A. C., Bassett, C., Lawson, G. L., and Jech, J. M. 2017. Exploiting signal processing approaches for broadband echosounders. ICES Journal of Marine Science, 74: 2262–2275.

Lunde, P., and Korneliussen, R. J. 2016. Power-budget equations and calibration factors for fish abundance estimation using scientific echo sounder and sonar systems. Journal of Marine Science and Engineering, 4: 10.3390.

Macaulay, G. J., Scoulding, B., Ona, E., and Fässler, S. 2018. Comparisons of echo-integration performance from two multiplexed echosounders. ICES Journal of Marine Science, 75: 2276–2285.

MacLennan, D. N., Fernandes, P. G., and Dalen, J. 2002. A consistent approach to definitions and symbols in fisheries acoustics. ICES Journal of Marine Science, 59: 365–369.

McClatchie, S., and Coombs, R. F. 2005. Low target strength fish in mixed species assemblages: the case of orange roughy. Fisheries Research, 72: 185–192.

McKelvey, D., and Lauffenberger, N. 2017. Results of the March 2016 acoustic-trawl survey of walleye pollock (*Gadus chalcogrammus*) conducted in the southeastern Aleutian Basin near Bogoslof Island, Cruise DY2016-03. AFSC Processed Report, 2017-11. 48 pp.

Miller, T. J. 2013. A comparison of hierarchical models for relative catch efficiency based on paired-gear data for US Northwest Atlantic fish stocks. Canadian Journal of Fisheries and Aquatic Sciences, 70: 1306–1316.

Moriarty, M., Sell, A. F., Trenkel, V. M., Lynam, C. P., Burns, F., Clarke, E. D., and Greenstreet, S. P. R. 2018. Resolution of biodiversity and assemblage structure in demersal fisheries surveys: the role of tow duration. ICES Journal of Marine Science, 75: 1672–1681.

National Research Council. 1998. Improving Fish Stock Assessments. The National Academies Press, Washington, DC. 177 pp.

Ona, E., Godø, O. R., Handegard, N. O., Hjellvik, V., Patel, R., and Pedersen, G. 2007. Silent research vessels are not quiet. Journal of the Acoustical Society of America, 121: 145–150.

Proud, R., Cox, M. J., and Brierley, A. S. 2017. Biogeography of the global ocean's mesopelagic zone. Current Biology, 27: 113–119.

Renfree, J. S., and Demer, D. A. 2016. Optimizing transmit interval and logging range while avoiding aliased seabed echoes. ICES Journal of Marine Science, 73: 1955–1964.

Simmonds, E. J., and MacLennan, D. N. 2005. Fisheries Acoustics, 2nd edn. Blackwell Science LTD, Oxford. 437 pp.

Stenevik, E. K., Vølstad, J. H., Høines, Å., Aanes, S., Óskarsson, G. J., Arge Jacobsen, J. A., and Tangen, Ø. 2015. Precision in estimates of density and biomass of Norwegian spring-spawning herring based on acoustic surveys. Marine Biology Research, 11: 449–461.

Stienessen, S., McCarthy, A., Jones, D., and Honkalehto, T. 2017. Results of the acoustic-trawl surveys of walleye pollock (*Gadus chalcogrammus*) in the Gulf of Alaska, February–March 2016 (DY2016-02 and DY2016-04). AFSC Processed Report, 2017-02. 91 pp.

Tichy, F. E., Solli, H., and Kaveness, H. 2003. Non-linear effects in a 200-kHz sound beam and the consequences for target strength measurement. ICES Journal of Marine Science, 60: 571–574.

Towler, R. H. 2017. Echolab MATLAB based EK60 library [Computer software]. https://bitbucket.org/afsc_mace/matlab-echolab/src/master/

Williams, K., Punt, A. E., Wilson, C. D., and Horne, J. K. 2011. Length-selective retention of walleye pollock, *Theragra chalcogramma*, by midwater trawls. ICES Journal of Marine Science, 68: 119–129.

Handling editor: Purnima Ratilal